Available online at www.sciencedirect.com

ScienceDirect

Procedia Engineering 105 (2015) 504 – 511

Procedia Engineering

www.elsevier.com/locate/procedia

6th BSME International Conference on Thermal Engineering (ICTE 2014)

Numerical modeling of Biomass co-combustion with pulverized coal in a small scale furnace

Arafat A. Bhuiyan and Jamal Naser*

Faculty of Science, Engineering and Technology (FSET)
Swinburne University of Technology, VIC-3122, Australia

Abstract

Co-combustion of Biomass is a promising greenhouse gases (GHG) abatement technology. This study presents a numerical modeling of co-combustion of coal and Biomass firing under air and oxy-fuel conditions in a small scale furnace. Co-firing conditions are varied with the Biomass sharing considering 20%, 40% on mass basis. Level of confidence is achieved by comparing the model-predicted peak radiative heat flux against the experimental data. Results are presented comparing the flame temperature distribution, species concentration for different cases. Unburned Carbon in ash (CIA) is predicted for different cases and reasonable agreement has been obtained. An improved burnout was observed in oxy-fuel cases. No significant change in CO_2 concentrations with the increase of biomass contribution to the total fuel input proves that biomass is CO_2-neutral energy source.

Peer-review under responsibility of organizing committee of the 6th BSME International Conference on Thermal Engineering (ICTE 2014)

Keywords: Co-combustion, Biomass, Oxy-fuel, Carbon in ash (CIA), Recycled Ratio (RR), Computational Fluid Dynamics (CFD).

1. Introduction

Co-combustion of Biomass with coal deals significant option for the reduction of greenhouse gas emissions specially the reduction of carbon dioxide (CO_2) emissions [1]. Co-combustion of Biomass with fossil fuel also increase the use of renewable based energy sources in energy systems [2]. On the other hand, oxy-fuel combustion is a proven carbon capturing technology [3]. In order to increase the CO_2 capture efficiency, the combination of oxy-fuel technology with Biomass co-firing is an interesting scope to investigate. In recent years, many efforts have been

* Corresponding author. Tel.: +61 3 9214 8655; fax: +61 3 9214 8264.
E-mail address: jnaser@swin.edu.au

Peer-review under responsibility of organizing committee of the 6th BSME International Conference on Thermal Engineering (ICTE 2014)
doi:10.1016/j.proeng.2015.05.083

conducted to investigate the effects of co-combustion of various types of Biomass in the existing small and large scale industrial furnace [1, 4-7]. Those results showed that co-combustion is technically feasible provided that agglomeration problems could be confronted. It is essential to model co-combustion in order to discover potential problems that may occur during Biomass co-firing and to mitigate potential negative effects of Biomass, including lower efficiency due to lower burnout. In this study, a comprehensive investigation has been carried out considering co-combustion of biofuel with coal under air-fuel and oxy-fuel conditions in a small scale furnace using a commercial computational fluid dynamics code AVL Fire ver.2009.2.

2. Model description and methodology

2.1. Geometry and operating condition of the boiler

This computational fluid dynamics (CFD) study is conducted simulating a small scale furnace. The dimensions and specifications of this refractory lined furnace are given in details in [8-10]. The furnace is equipped by an aerodynamically air staged burner with swirling facilities for proper mixing of the fuel and oxidizers [11]. Figure 1 shows the schematic representation of the combustion test facility used in this numerical study. In this study, Shea meal as a Biomass is co-fired with Russian coal as in the experiment [8]. The fuels properties are given in Table 1. Different co-firing ratios are considered on mass basis such as 20% and 40% Biomass sharing. Different oxy-fuel conditions are studied based on recycled ratios (RR) and compared with the air-firing case. Total three RR cases are considered in the range of 68-75%. The details of the applied boundary conditions are given in Table 2. The fuel particles size ranges in 75μm ->300μm for both fuels. But, larger particles are comparatively higher in biomass fuel.

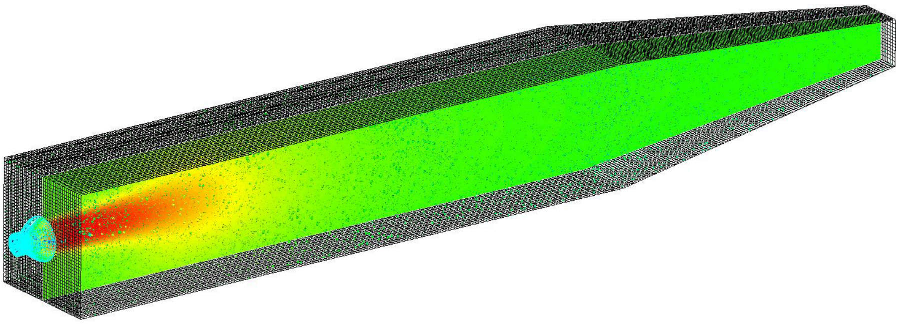

Figure 1: Schematic representation of the combustion test facility used in the numerical study.

Table 1: Proximate and ultimate analysis of the used fuels [12]

Fuel	Proximate analysis, (% as received)				Ultimate analysis, (% as received)					GCV MJ/kg
	VM	FC	Ash	Moisture	C	H	N	S	O	
Coal	33.55	48.27	11.98	6.23	65.91	4.59	2.09	0.34	8.89	27.098
Biomass	56.47	27.26	4.72	11.58	44.58	5.88	2.60	0.24	38.43	17.362

Table 2: Inlet Boundary condition applied to the burner

Flow parameters	Primary Oxidizer				Secondary Oxidizer			
	Air	RR75	RR72	RR68	Air	RR75	RR72	RR68
Gas flow, kg/h	110	155	155	155	620	600	512	424
Gas Temperature, K	343	343	343	343	543	543	543	543
O2 fraction, (kg/kg)	23.3	16.2	16.2	16.2	23.3	22.8	25.4	32.5

2.2. Numerical description

In this study, CFD is the main workhorse. The details numerical modeling used in this study are based on one of the author's previous work [11-13]. The mathematical model includes Eulerian-lagrangian gas and particulate phase modelling. In fuels combustion modelling, two important processes called devolatilisation and char oxidation are written as user-defined routines having different kinematics and coupled with the CFD code. In this study, Biomass particles are assumed in irregular shape while coal particles are assumed as spherical particle. In order to consider these effects, proper aerodynamics of the irregular shaped particles is taken into account by a user-defined drag correlation given in [14]. Regarding turbulence, k-ε turbulence model is considered [11-13, 15-18]. The reaction rate is determined by the Eddy-Breakup model [19]. In case of chemical reactions, multi-steps mechanisms have been introduced. For devolatilisation process, three steps homogeneous reactions are considered, but for char oxidation process, two-steps heterogeneous reaction mechanism is applied. In this study, SIMPLE algorithm is used for pressure velocity coupling. A standard convergence criterion of absolute residual 10^{-4} is considered. For the total duration of 80 s, time steps 0.0025 s was settled and the results were averaged after achieving quasi-steady state for all the variables. A 3-D non-uniform structured grid with 650,000 cells was adopted for the study.

3. Results and discussion

In this study, three different recycled ratios (RR) have been considered such as RR68, RR72 and RR75 cases. Results were presented and compared with the air-firing case. The effects of Biomass shares in co-firing (20% and 40% sharing of Biomass), firing conditions (see Table 2), and different fuels properties (see Table 1) have significant contribution to the overall performance of the furnace that are investigated and discussed in the following sections. For validation of the numerical work, peak radiative heat flux were predicted for different cases and compared with the available experimental work [8]. The comparison of the numerical and experimental peak radiative heat transfer measurement were presented in Table 5. It is found that the error percentage is very low in most of the cases.

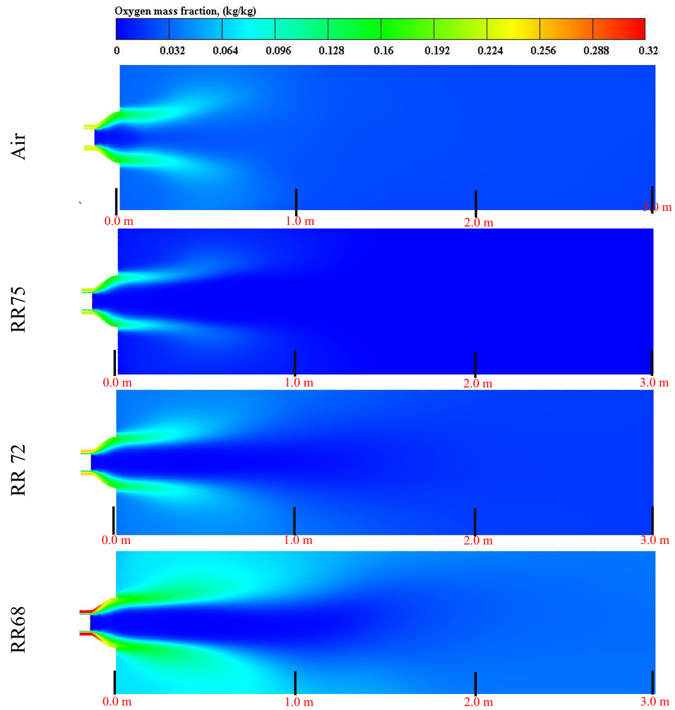

Figure 2: Oxygen mass fraction distribution on the horizontal plane for different cases considered (40% Biomass sharing).

Table 3: Comparison of numerical and experimental peak radiative heat transfer measurement

Cases	Coal+20% Biomass			Coal+40% Biomass		
	Experiment, KW/m^2	Prediction, KW/m^2	Error, %	Experiment, KW/m^2	Prediction, KW/m^2	Error, %
Air	385	395.36	2.69	395	360.56	8.71
RR75	328	318.90	2.77	--	294.77	--
RR72	375	380.97	1.59	328	340.99	3.96
RR68	435	437.85	0.65	370	386.67	4.50

Table 4: Prediction of numerical mean and furnace exit temperature for different cases

Cases	Coal+20% Biomass		Coal+40% Biomass	
	Mean Temp, K	Exit Temp, K	Mean Temp, K	Exit Temp, K
Air	1655.76	1338.62	1618.26	1333.26
RR75	1639.10	1328.94	1621.30	1328.94
RR72	1676.50	1332.38	1667.00	1328.16
RR68	1765.00	1422.70	1750.00	1414.65

The distributions of major oxidizing element (O_2) for different cases are presented in figure 2. From the figure, it is found that the peak value of the O_2 mass fraction is observed in the burner area. The maximum O_2 mass fraction in RR68 case is approximately 0.32 kg/kg. It is also seen that with the decrease of recycled ratio (RR), the mass fraction of O_2 is increased. This is in line with the applied boundary condition in table 2. As oxygen (O_2) mass fraction in increasing, accurate mixing of the fuels particle with the oxidizer is achieved, thus complete devolatilisation occurred. After devolatilisation, remaining amount of O_2 element reacts slowly with the char particle. This is the reason to form higher flame temperature having higher O_2 mass fraction in lower RR cases.

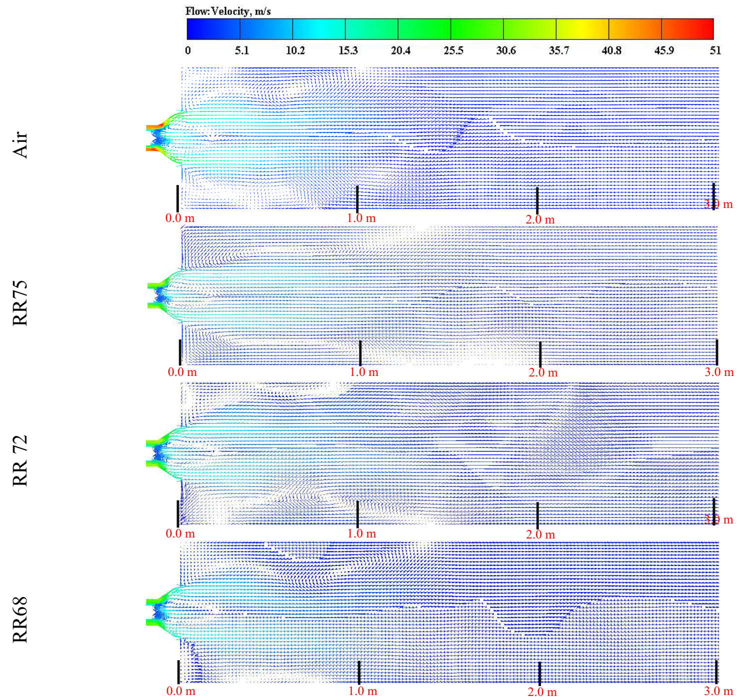

Figure 3: Axial velocity distribution (m/s) on the horizontal plane for different cases considered (40% Biomass sharing)

Axial velocity distributions for different cases considered in this study are presented in figure 3. This figure is representing for 40% sharing of Biomass co-combustion. From this figure, it is found that there are reaction zone after the exit of the burner where flames are expected to be found. Also, some internal and external recirculation zones are observed in various positions for all the cases. The position of external recirculation zone varies due to variation of flow conditions presented in table 2.With the increase of RR, flow velocity is increased, which will permit the fuel particles passing the reaction zone quickly. With the decrease of RR, flow becomes low which allow the fuel to stay in the reaction zone in more time. Thus volatile matters burn completely resulting higher flame temperature in lower RR.

The flame temperature distributions for different co-combustion ratio under different combustion environment on horizontal plane along the center of the furnace are presented in figures 4-7. These figures highlight the effects of variation of Biomass sharing in respective combustion cases. Biomass contains higher volatile contents compared to coal. So, in case of air-firing, Biomass burns early in the furnace because of the presence of highly volatile matters. With the increase of Biomass sharing in 40% case, the flame temperature expands more compared to 20% sharing because of higher percentage of volatile contents for all the cases. Though higher amount of volatile contents correspond to larger volume of flame in RR cases, but higher moisture content and larger particle sizes of Biomass tend to decrease the peak flame temperature. In this study, furnace exit temperature are predicted at a position of 4.2m from burner exit while mean flame temperature are predicted at 0.3m from burner exit. The furnace exit temperature and mean flame temperatures for different cases considering different Biomass sharing are presented in table 4. With the decrease of RR, mean flame temperature and furnace exit temperature increases. While considering increase of Biomass sharing from 20% to 40%, all the temperatures are lower in respective cases.

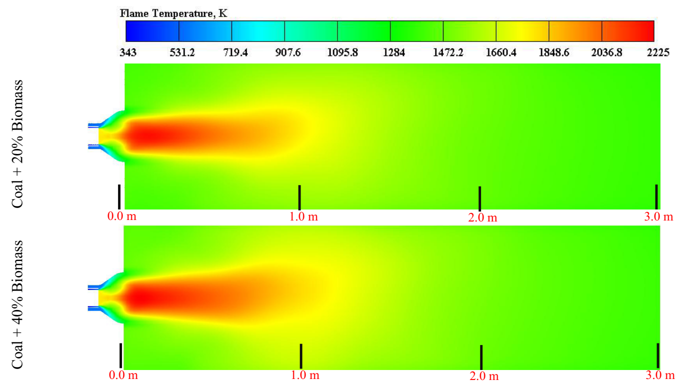

Figure 4: Flame temperature distribution on the horizontal plane for different Biomass sharing under air firing case.

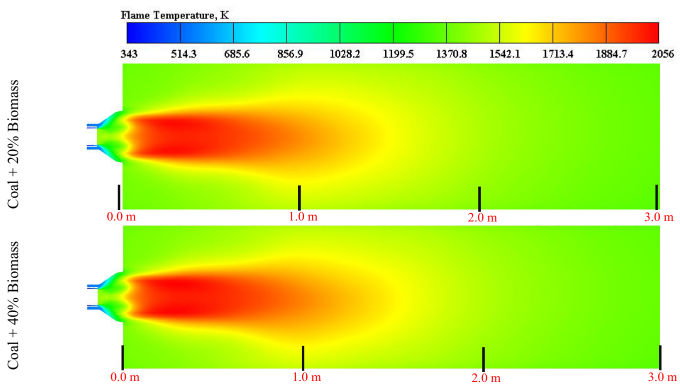

Figure 5: Flame temperature distribution on the horizontal plane for different Biomass sharing under oxy-firing (RR 75%) case.

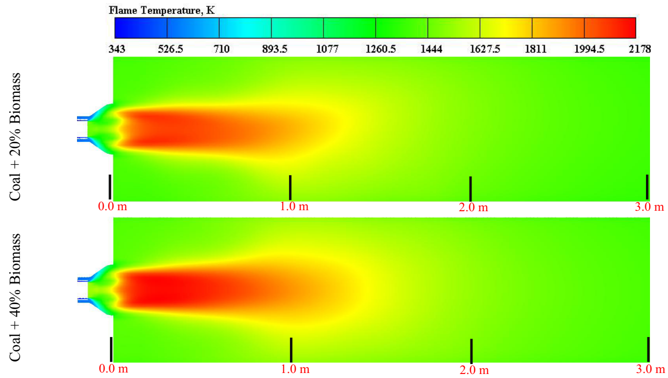

Figure 6: Flame temperature distribution on the horizontal plane for different Biomass sharing under oxy-firing (RR 72%) case.

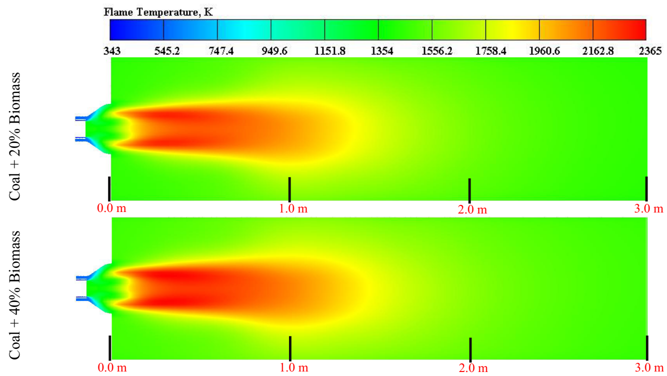

Figure 7: Flame temperature distribution on the horizontal plane for different Biomass sharing under oxy-firing (RR 68%) case.

Species mass fraction distribution for all the cases are presented in figure 8. Due to page limitations, results only for the 20% Biomass case are presented in this paper. Different species concentration such as (a).Carbon dioxide (CO_2), (b). Carbon monoxide (CO), (c). Hydrocarbon (CH_4), (d). Water vapour (H_2O) and (e). Hydrogen (H_2) mass fraction distributions are presented along the centre of the furnace from the exit of the burner under different combustion environment. Figure 10(a) represents the distributions of the CO_2 formation inside the furnace. From the figure it is found that for air firing case, CO_2 formation is below 20%. When transferred to oxy-firing cases, CO2 formation increases to 70-90% ranges. With the decrease of RR, maximum value of CO_2 is decreasing. Also, it is found in this study that with the increase of Biomass sharing, no significant changes for the formation of CO_2 is observed. So, it can be concluded that usage of Biomass is CO_2 neutral and fossil fuel can be totally replaced by the Biomass or partially replaced by increasing the Biomass sharing depending on the expected energy. In heterogeneous chemical process, CO is formed after the intermediate reaction of char with oxidizer which further produces emissions. CO distribution is shown in figure 8(b) for different cases. In this study, the hydrocarbon product from the devolatilisation is considered as equivalent to CH_4. Hydrocarbon (HC) mass fraction distribution is presented in Figure 10(c). When CO_2 concentration is low and O_2 concentration is high at RR68 case, peak of the HC is seen near the burner exit. With the increase of RR, HC mass fraction tends to zero. The formation of hydrogen (H_2) and water vapour (H_2O) mass fraction is related. With the decrease of RR, H_2 and H_2O both increase. While compared to air-firing case, increase in each mass fraction is found for all oxy-fuel cases. These are presented in figure 8(d) & (e) for H_2O and H_2 mass fraction distributions respectively. Prediction of Carbon in Ash (CIA) is an important achievement in this numerical study. Accurate prediction of CIA is a significant measure to determine the efficiency of Biomass co-combustion in a power plant. Figure 9 shows the comparison of numerical prediction and experimental measurement of Carbon-in-Ash (CIA). This prediction is only a qualitative measure. But overall, reasonable agreement has been observed between the numerical and the experimental data.

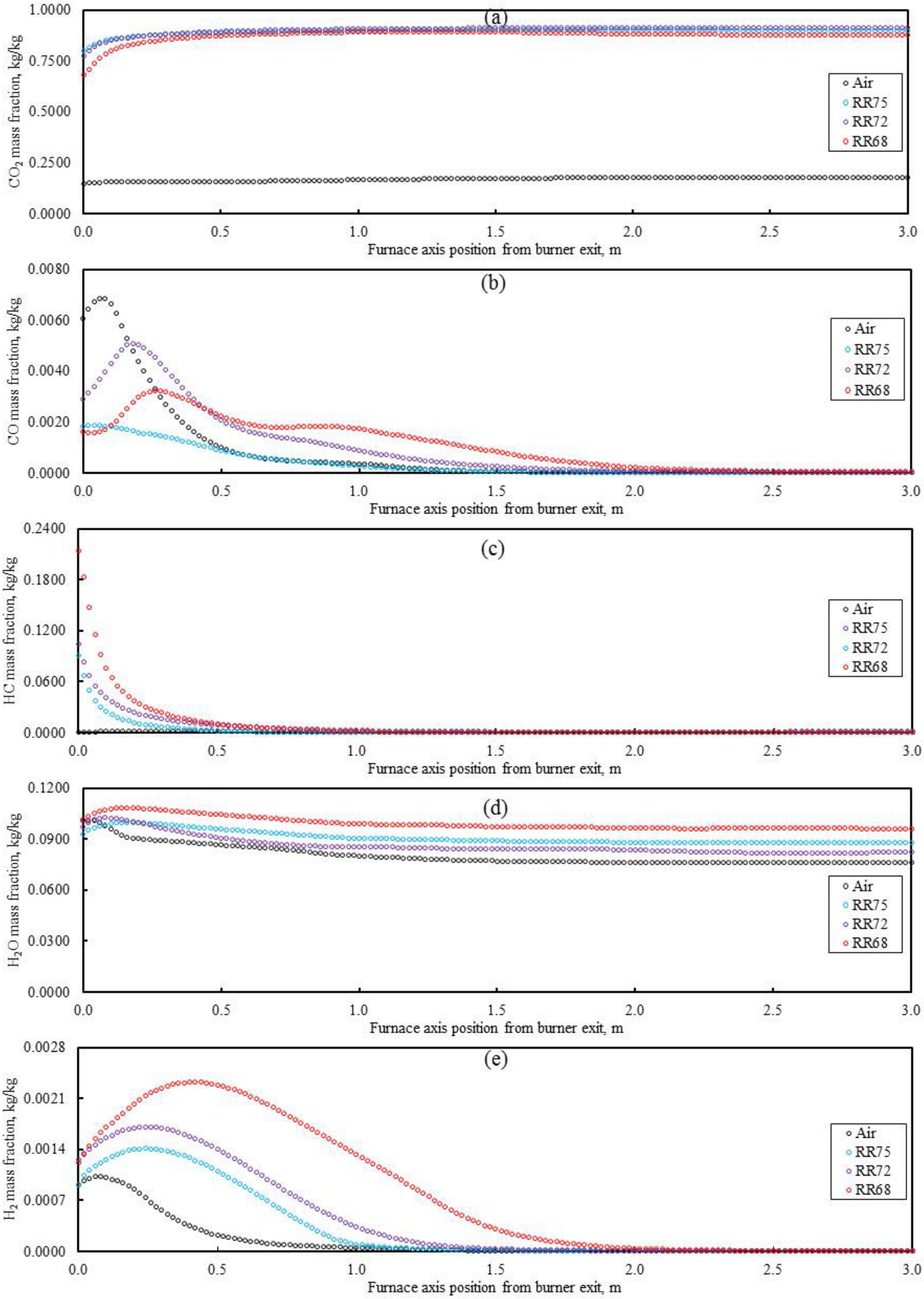

Figure 8: Species mass fraction distribution on axial direction for 20% Biomass sharing for different combustion environment.

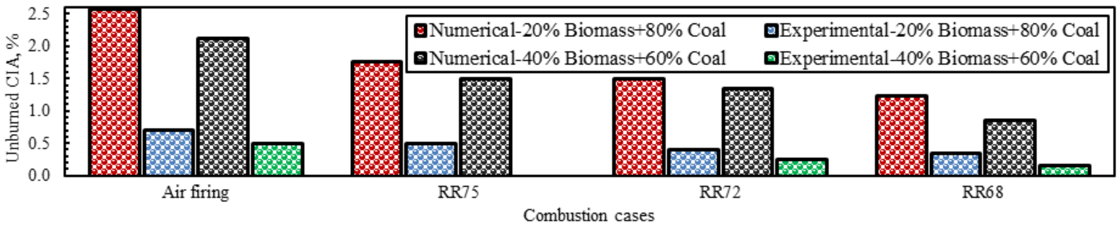

Figure 9: Comparison of numerical and experimental CIA measurement in different oxy-fuel co-firing conditions

Conclusion

Numerical modelling of Biomass co-combustion has been conducted considering Shea meal as a Biomass co-fired with Russian coal in a small scale furnace. In this study, different co-firing ratio such as 20% and 40% Biomass sharing has been investigated. A commercial CFD code coupled with some user defined program is incorporated to carry out the investigation. Grid sensitivity test has been conducted for a reference air firing case and the code was validated with the available experimental data. Results are presented for different combustion environment including air-firing and oxy-fuel combustion cases. The highlight of this study is to differentiate the effects of biomass sharing on the overall flame temperature. Also, related combustion species such as oxygen, carbon dioxide, carbon monoxide, hydrogen, water vapour, and hydrocarbon mass fraction distribution inside the furnace is identified. Furnace exit temperature and mean flame characteristics with the change of fuel ratio and flow condition has been studied. Finally, unburned Carbon in ash is predicted for all the cases and a reasonable agreement has been obtained.

Reference

1. Baxter, L., Biomass-coal co-combustion: opportunity for affordable renewable energy. Fuel, 2005. 84(10): p. 1295-1302.
2. Demirbas, A., Combustion characteristics of different biomass fuels. Progress in energy and combustion science, 2004. 30(2): p. 219-230.
3. Scheffknecht, G., et al., Oxy-fuel coal combustion—A review of the current state-of-the-art. International Journal of Greenhouse Gas Control, 2011. 5: p. S16-S35.
4. Haykiri-Acma, H., S. Yaman, and S. Kucukbayrak, Co-combustion of low rank coal/waste biomass blends using dry air or oxygen. Applied Thermal Engineering, 2013. 50(1): p. 251-259.
5. Sarabèr, A., Co-combustion and its impact on fly ash quality; pilot-scale experiments. Fuel Processing Technology, 2012. 104(0): p. 105-114.
6. Bragato, M., et al., Combustion of coal, bagasse and blends thereof: Part I: Emissions from batch combustion of fixed beds of fuels. Fuel, 2012. 96(0): p. 43-50.
7. Nussbaumer, T., Combustion and co-combustion of biomass: fundamentals, technologies, and primary measures for emission reduction. Energy & Fuels, 2003. 17(6): p. 1510-1521.
8. Smart, J.P., R. Patel, and G.S. Riley, Oxy-fuel combustion of coal and biomass, the effect on radiative and convective heat transfer and burnout. Combustion and Flame, 2010. 157(12): p. 2230-2240.
9. Smart, J.P., P. O'Nions, and G.S. Riley, Radiation and convective heat transfer, and burnout in oxy-coal combustion. Fuel, 2010. 89(9): p. 2468-2476.
10. Smart, J., et al., Characterisation of an oxy-coal flame through digital imaging. Combustion and Flame, 2010. 157(6): p. 1132-1139.
11. Bhuiyan, A.A. and J. Naser, Numerical modelling of oxy fuel combustion, the effect of radiative and convective heat transfer and burnout. Fuel, 2015. 139(0): p. 268-284.
12. Bhuiyan, A.A. and J. Naser, Computational modelling of co-firing of biomass with coal under oxy-fuel condition in a small scale furnace. Fuel, 2015. 143(0): p. 455-466.
13. Bhuiyan, A.A. and J. Naser. Effect of recycled ratio on heat transfer performance of coal combustion in a 0.5MWth combustion test facility. in 19th Australasian Fluid Mechanics Conference Melbourne, Australia. 2014.
14. Haider, A. and O. Levenspiel, Drag coefficient and terminal velocity of spherical and nonspherical particles. Powder Technology, 1989. 58(1): p. 63-70.
15. Bhuiyan, A.A., et al., Plate fin and tube heat exchanger modeling: Effects of performance parameters for turbulent flow regime. International Journal of Automotive and Mechanical Engineering, 2014. 9(1): p. 1768-1781.
16. Bhuiyan, A.A., M.R. Amin, and A.S. Islam, Three-dimensional performance analysis of plain fin tube heat exchangers in transitional regime. Applied Thermal Engineering, 2013. 50(1): p. 445-454.
17. Bhuiyan, A., A. Islam, and M. Amin, Numerical study of 3D thermal and hydraulic characteristics of wavy fin-and-tube heat exchanger. Frontiers in Heat and Mass Transfer (FHMT), 2012. 3(3).
18. Bhuiyan, A.A., A.S. Islam, and M.R. Amin, Numerical Prediction of Laminar Characteristics of Fluid Flow and Heat Transfer in Finned-Tube Heat Exchangers. Innovative Systems Design and Engineering, 2011. 2(6): p. 1-12.
19. Spalding, D.B., Mixing and chemical reaction in steady confined turbulent flames. Symposium (International) on Combustion, 1971. 13(1): p. 649-657.